Dehydrogenation and the surface phase transition on diamond (111): Kinetics and electronic structure

J. B. Cui, J. Ristein, and L. Ley
Institute of Technical Physics, University of Erlangen-Nürnberg, Erwin-Rommel-Strasse 1, D-91058 Erlangen, Germany
(Received 27 July 1998; revised manuscript received 8 September 1998)

The (1×1) to (2×1) surface phase transition of the hydrogen-covered diamond (111) surface is investigated by core level spectroscopy, low-energy electron diffraction, and measurements of the electron affinity. The latter method is shown to be a reliable measure of the hydrogen coverage. Prolonged annealing of the surface at 1000 K converts the hydrogen-terminated (1×1) structure with an electron affinity of -1.27 eV to a hydrogen-free (2×1) reconstruction, increases the separation of valence-band maximum from the Fermi level E_F from 0.68 to 0.88 eV, and results in a positive electron affinity of $+0.38$ eV. Annealing the surface at high temperature (up to 1400 K) yields the same (2×1) surface structure albeit with an increase in the separation of the valence-band maximum from E_F to 1.42 eV and a positive electron affinity of 0.8 eV which is associated with a partial surface graphitization. An analysis of the kinetics of the thermally induced hydrogen desorption yields an activation energy of 1.25 ± 0.2 eV. It was found that hydrogen desorption and reconstruction are surface phase transitions which are not directly linked. Instead, an intermediate phase with a high concentration of dangling bonds (up to 70%) is observed. The (1×1) to (2×1) phase transition is phenomenologically well described by a first-order transition provided a critical density of dangling bonds of about 70% is included in the analysis in such a way that the rate constant for reconstruction vanishes below that value. [S0163-1829(99)10407-7]

I. INTRODUCTION

From a technological and scientific point of view the most important surfaces of diamond are the low-index (111) and (100) surfaces. They account for the majority of the facets in polycrystalline chemical vapor deposition (CVD) diamond films. Depending on the hydrogen coverage these surfaces exhibit different reconstructions.[1–6] The (2×1) reconstruction of the clean diamond (111) surface is usually described in terms of the π-bonded chain model of Pandey[7] which has been successfully applied to describe the surface band structure of diamond (111) (2×1).[8] The hydrogen-terminated diamond (111) surface has a bulklike (1×1) structure and each carbon atom on the topmost layer is supposed to be terminated by one hydrogen atom.

The structural transformation from a hydrogenated (1×1) to the hydrogen-free (2×1) reconstruction accompanying the H desorption is reported to occur after annealing at temperatures above 950 °C.[9] At the same time the surface band bending also changes. The bulk Fermi level for type-IIb semiconducting diamond normally lies 0.2–0.4 eV above the valence-band maximum (VBM) depending on the acceptor concentration and that of compensating donors. On the hydrogen-terminated type-IIb diamond the band diagram extends with no or little downward band bending to the surface.[10] After hydrogen desorption and surface reconstruction at high temperature a large downward band bending is often observed by photoelectron emission spectroscopy with the surface Fermi level positioned 1.2–1.6 eV above the surface VBM.[10,11] In our recent mild surface annealing experiment at a temperature of 727 °C, however, a stable Fermi level position of 0.88 eV above the surface VBM was measured for the (2×1) reconstructed diamond (111) surface.[12]

Apart from these differences between the hydrogen-terminated and clean diamond (111) surfaces, a change in the sign of the electron affinity χ is observed. The electron affinity of a semiconductor is defined as the energy difference between the vacuum level $E_{\rm vac}$ and the conduction-band minimum (CBM) E_C: $\chi = E_{\rm vac} - E_C$. Depending on the sign of χ one refers to the surface as having positive or negative electron affinity (PEA or NEA). The magnitude of the electron affinity as described above is closely related to the kinds of adsorbates on the diamond surface. The clean (2×1) reconstructed as well as the oxygenated diamond (111) surfaces show PEA while the hydrogen-terminated (1×1) surface exhibits NEA.[12,13,14]

Considering the considerable number of publications concerned with one or the other aspect of the dehydrogenation process and the reconstruction of the diamond (111) surface one might ask, why another study? The present study differs from the previous ones in several important aspects. (i) It applies a large number of UHV-compatible techniques simultaneously in order to characterize the state of the surface and its electronic structure as completely as possible. These are low-energy electron diffraction (LEED) and C 1*s* core level studies to monitor the structural arrangement and the chemical bonds of the surface atoms; work function measurements with a Kelvin probe and total photoelectron yield spectroscopy provide in combination with the C 1*s* binding energies information about electron affinity and surface band bending; the electron affinity furthermore is shown to be a measure of the hydrogen coverage. (ii) We induce the phase transition from the hydrogenated (1×1) to the hydrogen-free (2×1) surface by isothermal annealing at 1000 K as well as by isochronal annealing at increasing temperatures using the same sample. This comparison provides insight

into the kinetics of hydrogen desorption and reconstruction and clarifies some of the existing inconsistencies concerning surface band bending as the result of dehydrogenation and reconstruction. (iii) In our analysis we do not assume that the (2×1) reconstruction follows directly from the dehydrogenation but allow for an intermediate state in which surface atoms are neither bonded to hydrogen nor involved in the reconstruction. (iv) Last but not least, we utilize a reliable method to measure the true temperature of the diamond sample with an accuracy of ±10 K. In conjunction with the comparison mentioned under (ii) this turns out to be crucial in the attempt to sort out some of the contradictions concerning the kinetics of hydrogen desorption and reconstruction that have recently been recorded.[15–20]

II. EXPERIMENTAL DETAILS

A. Sample preparation and temperature measurement

The sample used in this study was a natural type-IIb diamond (111) single crystal with surface dimensions of 3×5 mm^2. The boron concentration of the sample was about 10^{16} cm^{-3} and the conductivity of the order of $1\ \Omega^{-1}$ cm^{-1} which is sufficient to avoid any surface charging in our measurements. From the boron concentration and the energy of the acceptor level (0.36 eV) the Fermi level position in the bulk is calculated to lie 0.32 ± 0.01 eV above the VBM, allowing for a compensation ratio of 0 to 0.2. The as-received diamond surface had been mechanically and hydrogen plasma polished. After an anneal under UHV conditions at 1400 K for 12 min to desorb surface contamination and hydrogen it was treated in a hydrogen plasma at about 1100 K for 10 min to provide a controlled surface hydrogenation. This process produces not only a hydrogen termination of the surface but also clean and atomically flat surfaces.[21,22] The so treated diamond surface showed a sharp (1×1) LEED pattern and an ordered surface structure as indicated by the prominence of strong dispersion features in the angle-resolved photoemission spectra.[8] On the surfaces used for the isothermal annealing (referred to as surface A), no contaminants were found by x-ray excited photoemission spectroscopy (XPS) while about 7% of a monolayer of oxygen was detected on the surface used for the isochronal annealing sequence (surface B).

The diamond samples were clamped to a Ta foil which was heated by electron bombardment from the back. The temperature of the diamond sample was measured by a newly developed method which is based on the Raman line position of diamond and yields the temperature of diamond itself and not that of the sample holder with an accuracy of ±10 K.[23]

B. Surface characterization

The diamond surfaces were characterized by XPS, LEED, and total photoelectron yield spectroscopy. A monochromatized Al $K\alpha$ x-ray source with a photon energy of 1486.6 eV was used to excite C 1s core level photoelectron emission. The combined resolution of light source and analyzer is 0.6 eV for the XPS measurements. The surface band bending was monitored by the binding energy of the C 1s level relative to the Fermi level which has been measured with an accuracy of ±0.06 eV. The work function of diamond was measured by the contact potential difference (CPD) between the diamond sample and a gold foil using the Kelvin method.[24] The work function of the gold foil was in turn determined by fitting a Fowler function to its photoelectric yield spectrum. This method gives an accuracy in the CPD of ±10 meV and of ±30 meV for the work function of diamond. The total photoelectron yield spectra were measured by the setup described in Ref. 25. All measurements were performed on the diamond surfaces that were allowed to cool down to room temperature after each annealing step in the UHV chamber with a base pressure of about 10^{-8} Pa.

III. RESULTS

A. Isothermal annealing at 1000 K

The experiment proceeds as follows. After hydrogenation the CPD, the C 1s core level spectrum, and LEED are measured. Then the sample with surface A is taken in a few steps up to 1000 K. At this temperature the sample is kept for a finite amount of time, then cooled down to room temperature, and CPD, XPS, and the yield spectrum are measured and the reconstruction of the surface is monitored by LEED. Repeating these steps and annealing the sample thus for a total of 12 000 sec at 1000 K the hydrogen is desorbed and the surface transforms from a (1×1) surface with NEA to a (2×1) reconstructed one with PEA.

The change in surface structure as monitored by LEED is shown in Fig. 1. The as-hydrogenated surface shows a sharp (1×1) LEED pattern [Fig. 1(a)] and a weak (2×1) reconstruction occurs after annealing at 1000 K for 2520 sec [Fig. 1(b)]. The fully (2×1) reconstructed surface is obtained by a 7200-sec anneal at 1000 K as shown in Fig. 1(c).

Figure 2 shows the C 1s core level spectral region of diamond (111) surfaces after hydrogen plasma treatment and annealed at 1000 K for 1440 and 9780 sec, respectively. The spectra were fitted by a Voigt function. The full width at the half maximum (FWHM) of the Lorentzian and Gaussian components was kept constant with values of 0.3 and 0.8 eV, respectively. In addition to the bulk C 1s peak at 284.8 eV two surface components shifted by $+0.8$ eV (S_A) and -1.03 eV (S_C) are observed. These surface components have been discussed by Graupner *et al.*[20] and S_A was assigned to the emission from carbon atoms bonded to more than one H atom at the surface. After 1440 sec annealing at 1000 K, the surface component S_A disappears [see Fig. 2(b)]. Upon further annealing the surface component S_C appears [Fig. 2(c)], which is associated with C atoms involved in the π bonds of the (2×1) surface reconstruction.[20] The intensity of this lower binding energy surface component S_C increases with annealing time and saturates after 7200 sec.

The change in the bulk C 1s binding energy with annealing time is given by the solid squares in Fig. 3(a). Between the as-hydrogenated state and the start of annealing at 1000 K the sample had already been annealed for a total of 28 min at various lower temperatures. To include the effects of this low-temperature annealing in the isothermal annealing sequence requires placing it in advance of the second data point by an effective time t_{eff} that would cause the same change as a single annealing step at 1000 K. Because t_{eff} depends on the kinetics of the process responsible for the

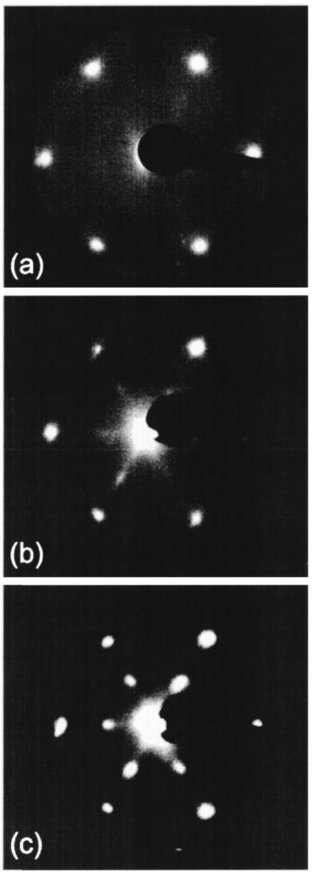

FIG. 1. LEED pattern of the diamond (111) surface as a function of annealing time at $T=1000\,\mathrm{K}$. (a) As hydrogenated, $E=102\,\mathrm{eV}$; (b) after 2520 sec, $E=117\,\mathrm{eV}$; (c) after 7200 sec, $E=117\,\mathrm{eV}$.

changes in binding energy and other properties we have just indicated upper (28 min) and lower (0 min) limits for t_{eff} by the length of the bar. The horizontal bar in the electron affinity plot of Fig. 3(c) has the same meaning. The binding energy increases by 0.2 eV in the first 2000 sec of annealing and levels off thereafter. This binding energy change is equivalent to an additional 0.2 eV in downward band bending on the diamond (111) surface (compare Sec. IV C).

As described above, the surface reconstruction is characterized by the half-order spots in the LEED patterns and by the lower binding energy C 1*s* surface component S_{C}. Figure 3(b) gives the ratio of the half- to first-order LEED spot intensities (left-hand scale) and the relative intensity of the C 1*s* surface component S_{C} $[I_{S_{\mathrm{C}}}/(I_{S_{\mathrm{C}}}+I_{\mathrm{bulk}})$, right-hand scale] as a function of annealing time. The intensities of LEED spots were directly measured from the LEED pattern and after averaging over the three (2×1) domains their ratios were normalized to the saturated value. The intensities of C 1*s* surface and bulk components were obtained from the least squares fits. It is safe to assume that the contribution of surface carbon atoms to the photoemission signal remains constant during the transformation of the surface structure from (1×1) to (2×1). Therefore, the relative intensity of surface component S_{C} is a measure of the change in reconstruction coverage. The intensity of the half-order LEED spots and that of the surface component S_{C} track each other perfectly. Both start to appear not earlier than after a total of

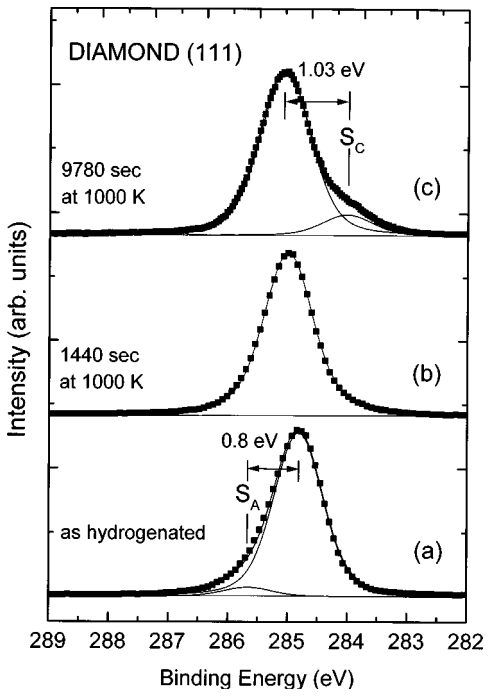

FIG. 2. C 1*s* core level spectra taken on diamond (111) surfaces as a function of annealing time at 1000 K. Solid squares are the experimental data and the lines are fits using Voigt functions. (a) The as-hydrogenated surface; (b) after 1440 sec; (c) after 7200 sec.

2100 sec of annealing and they saturate together after 7000 sec when the surface is fully (2×1) reconstructed.

The electron affinity χ can be expressed in terms of the work function ϕ, the Fermi level E_F, the top of the valence band E_V, and the energy gap E_g (5.47 eV at room temperature) as

$$\chi=E_{\mathrm{vac}}-E_C=\phi+(E_F-E_V)-E_g\,. \tag{1}$$

The top of the valence band is difficult to determine for diamond, in particular, during dehydrogenation when the VBM is masked by surface states.[8] We therefore determined first the change in electron affinity $\Delta\chi$ by measuring the change in work function $\Delta\phi$ and that in (E_F-E_V) simultaneously as a function of annealing time.

The work function of diamond was measured as explained in Sec. II B. Changes in (E_F-E_V) are in general changes in surface band bending that occur in the course of the hydrogen desorption. They were measured by following the binding energy of the C 1*s* core level relative to E_F because the C 1*s* level has a fixed energy separation from the valence-band maximum. The surface band bending extends over a distance ($\sim$150 nm) large compared to the probe depth ($\sim$2 nm) of photoemission.

In Fig. 3(c), we have plotted the variation in χ as a function of annealing time. The data points are derived from the CPD measurements and encompass the correction for changes in band bending. The initial value of χ corresponds to the nonannealed state. The electron affinity χ increases as the annealing time proceeds and it saturates after about 7200 sec annealing. The total change in χ is 1.65 eV.

The changes in χ which are directly measured are converted into absolute χ values by monitoring the transition from NEA to PEA using yield spectroscopy. Up to an an-

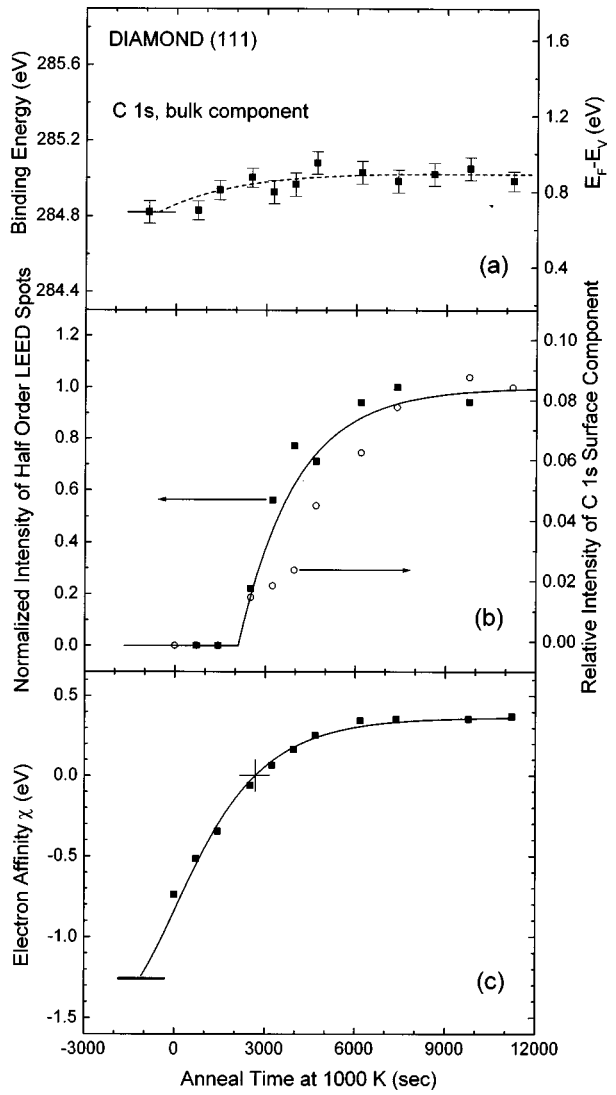

FIG. 3. (a) Binding energy of the C 1*s* bulk component; (b) relative intensity of the half-order LEED spots (solid squares) and that of the C 1*s* surface component S_C (open squares); (c) electron affinity χ as a function of annealing time at 1000 K. The solid line in (b) is the fit of experimental data points to Eq. (11) and the solid line in (c) is the fit using Eqs. (2) and (4). The cross in (c) indicates the transition point of the electron affinity from negative to positive.

nealing time of 2520 sec the yield spectra are characteristic for surfaces with NEA because the photoelectron yield rises sharply when the photon energy reaches the band gap of diamond at 5.47 eV which is a reliable fingerprint for NEA.[10,26] After 3240 sec of annealing the sudden rise of the photoelectron yield at E_g disappears because the vacuum level is now above E_C. We thus place the point corresponding to $\chi=0$ in the middle between the 2520 and 3240 sec annealing [cross in Fig. 3(c)]. In this way χ is referred to an absolute scale with an accuracy of ± 0.065 eV because the change in χ amounts to 0.13 eV between 2520 and 3240 sec of annealing.

B. Isochronal annealing

In a second series of experiments hydrogen desorption and the (1×1) to (2×1) phase transition were achieved by subjecting the hydrogenated sample to a series of isochronal annealing steps at increasing temperature up to 1420 K. The sample was kept at each temperature for 10 min and after cool down the same kinds of measurements were performed as for the isothermal annealing sequence. This kind of annealing was performed because it is more closely related to the temperature ramps normally used to desorb hydrogen from diamond surfaces.[20,27]

The pertinent results concerning the C 1*s* binding energy, the intensity of the half-order LEED spots, the relative intensity of the S_C surface component, and the electron affinity are collected in Fig. 4 in a form identical to that of Fig. 3. Because the sample is kept at each temperature for a time short compared to those of the isothermal annealing sequence, the (1×1) to (2×1) phase transition sets in at a slightly higher temperature, namely, 1050 K, and it is completed at 1150 K, as judged by the intensities of the half-order LEED spots which remain constant thereafter.

In fact at this temperature marked by the vertical line in Fig. 4 the other indicators, such as surface Fermi level position ($E_F-E_V\approx 0.9$ eV), the relative intensity of the S_C component (≈ 0.09), and the electron affinity ($\chi\approx 0.4$ eV) also reach values identical to those attained at the end of the isothermal annealing sequence (Fig. 3). However, these quantities continue to increase— E_F-E_V and I_{S_C} even with a different slope —until E_F-E_V and χ reach a new equilibrium at about 1400 K.

IV. ANALYSIS AND DISCUSSION

A. The kinetics of hydrogen desorption

The surface dipole layer set up by the partially ionic C^-—H^+ bond lowers the electron affinity by 1.65 eV upon hydrogenation of the clean (111) surface.[12] Such a dipole layer causes a potential step ΔV perpendicular to the surface over a distance of the order of the C—H bond length of 1.1 Å. The reduction in χ from $\chi_{\max}$ is equal to $-e\Delta V$ which in turn depends on the areal density n and the magnitude p of the dipole moment of each C—H unit:

$$\chi-\chi_{\max}=-e\Delta V=-\frac{epn}{\varepsilon_0}g(n), \tag{2}$$

where ε_0 is the dielectric constant of free space. In this model the dipole density n equals the hydrogen density $f_H n_0$ on the diamond surface where $n_0=1.81\times10^{15}\,\mathrm{cm}^{-2}$ is the areal density of C atoms on the (111) surface. The function g which depends on n takes the interaction of dipoles into account with the result that the contribution of each dipole to ΔV is reduced for high dipole densities. An expression for $g(n)$ with the polarizability α of the dipoles as a parameter can be obtained according to the calculation of Topping:[28]

$$g(n)=\left(1+\frac{9\alpha n^{3/2}}{4\pi\varepsilon_0}\right)^{-1}. \tag{3}$$

The polarizability α for the C—H dipoles is $1.28\times10^{-40}\,As m^2/V$ which is calculated from the refractive index of polyethylene (1.5) using the Clausius-Mossotti relation.[29]

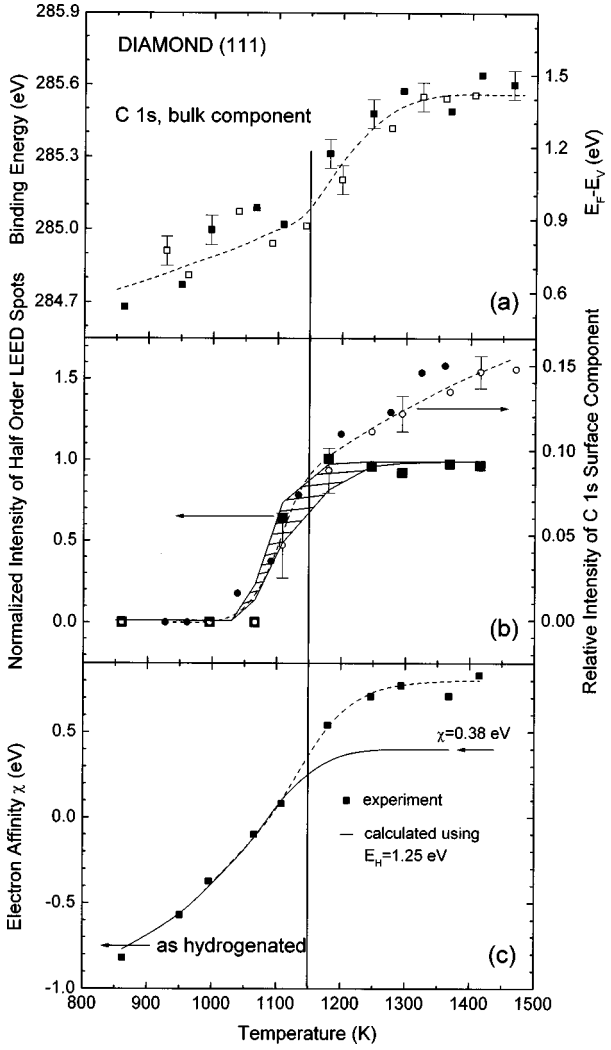

FIG. 4. (a) Binding energy of the C 1*s* bulk component; (b) relative intensity of half-order LEED spots (solid squares) and that of the C 1*s* surface component S_C (open and closed circles); (c) electron affinity χ as a function of annealing temperature. The dashed lines are guides to the eye. The solid and open squares in (a) and the closed and open circles in (b) stem from two independent series of experiments. The shaded band in (b) is the calculation using Eq. (13) with upper and lower limits for the parameters ν_R and α, and the solid line in (c) is a fit using Eqs. (7) and (2). In (c) the arrow at $\chi=+0.38$ eV indicates the saturation value of the electron affinity for the hydrogen-free (2×1) reconstructed surface as derived from the isothermal annealing sequence.

We assume, as is commonly done, that the hydrogen desorption is a first-order thermally activated process. Then for isothermal annealing at a constant temperature T the fraction f_H of the surface covered with hydrogen is given as a function of time t as

$$f_H(t)=f_H(0)e^{-A(T)t}. \tag{4}$$

The rate constant

$$A(T)=\nu_H e^{-E_H/kT} \tag{5}$$

is thermally activated with an activation energy E_H and a prefactor ν_H.

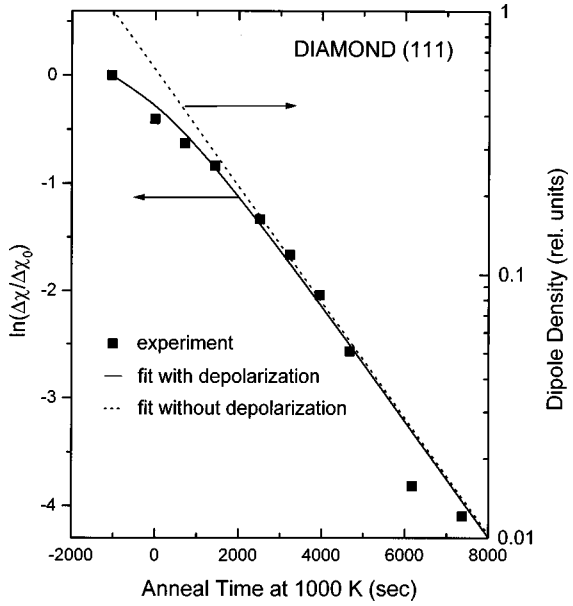

FIG. 5. Change in $\ln(\Delta\chi/\Delta\chi_0)$ as a function of annealing time. $\Delta\chi_0=1.65$ eV is the electron affinity difference between the as-hydrogenated and the hydrogen-free surface while $\Delta\chi$ is the difference between the surface annealed at a certain temperature and the hydrogen-free surface. The solid squares are the experimental data points. The solid and dashed lines are the calculated curves with and without taking depolarization effects into account, respectively. The dashed line corresponds simultaneously to the hydrogen coverage (right-hand scale).

By combining the expression for the surface hydrogen coverage as given by Eq. (4) with Eq. (2) the change $\Delta\chi(t)$ can be calculated using A and p as free parameters. The best fit result shown as a solid line in Fig. 3(c) is obtained with $A=5.4\pm0.2\times10^{-4}\,\mathrm{sec}^{-1}$ and $p=1.45\times10^{-30}Asm$.[30]

It should be pointed out that a satisfactory fit of the experimental $\Delta\chi(t)$ values to Eq. (2) is not possible without taking the depolarization into account. In the absence of depolarization, i.e., for $g(n)=1$, $\ln(\Delta\chi/\Delta\chi_0)$ is a linear function of annealing time as shown by the dashed line in Fig. 5. The experimental values as given by the solid squares in Fig. 5 do, however, deviate from the linear relationship in proportion to the H coverage, i.e., with decreasing annealing time a discrepancy occurs that is remedied when the depolarization is taken into account (solid line in Fig. 5). For the fully hydrogen-covered surface $g(n_0)=0.53$, that is, the effective dipole moment is reduced to half of its intrinsic value.

Turning now to the isochronal annealing we noticed in connection with Fig. 4 that both the S_C surface component intensity and the amount of band bending and electron affinity increased beyond the point where the (2×1) reconstruction is completed. The electron affinity and the surface Fermi level position saturate at about 1400 K at $\chi=0.8$ eV and $E_F-E_V=1.42$ eV, respectively. The C 1*s* surface component continues to grow over the whole range of the experiment with no significant saturation. For reasons to be discussed later this further phase transition and the accompanying change in the electronic structure of the surface are ascribed to a partial graphitization of the (111) surface. This implies that the increase in χ up to 0.38 eV is due

to hydrogen desorption and the further increase caused by the graphitization and not by a further hydrogen desorption process.

In the isochronal annealing mode the sample is taken through a series of annealing steps i such that the sample is kept at a T_i for periods of time Δt with $T_i > T_{i-1}$. In this case the rate equations can only be integrated for each isothermal annealing step i and recursion expressions follow which relate the hydrogen coverage $f_{\mathrm{H},i}$ at the end of step i to that at the end of previous annealing step $f_{\mathrm{H},i-1}$:

$$f_{\mathrm{H},i} = f_{\mathrm{H},i-1} e^{-A_i \Delta t}, \tag{6}$$

with $A_i = \nu_{\mathrm{H}} e^{-E_{\mathrm{H}}/kT_i}$. Summing over all steps from $i=0$ to some finite step k yields

$$f_{\mathrm{H},k} = f_{\mathrm{H},0} \exp\left(-\sum_{i=1}^{k} A_i \Delta t \right). \tag{7}$$

We have therefore fitted the measured change in χ for temperatures below 1200 K using Eq. (7) with the further proviso that the hydrogen-induced change in χ levels off at $+0.38$ eV in the limit of high temperatures. The best fit result shown by the solid line in Fig. 4(c) is obtained with a prefactor $\nu_{\mathrm{H}} = 1 \times 10^3\ \mathrm{sec}^{-1}$ and an activation energy for hydrogen desorption of $E_{\mathrm{H}} = 1.25$ eV. Naturally, these parameters for the hydrogen desorption process yield at 1000 K the rate constant A as it was derived from the analysis of the isothermal annealing process.

The activation energy E_{H} for H desorption agrees with that obtained by Schulberg, Kubiak, and Stulen[16] but is much lower than the 3.2 eV given by Thomas, Rudder, and Markunas[17] or the 3.5 eV by Yang *et al.*[18] Nishimori *et al.*[31] measured the desorption yield of H ions from a diamond (100) surface as a function of temperature and obtained an activation energy of 0.8 eV. Most of the high values for E_{H} are obtained by fitting experimental data using a fixed ν_{H} of about $10^{13}\ \mathrm{sec}^{-1}$. However, if E_{H} and ν_{H} are both kept as free parameters, low values of E_{H} and ν_{H} are obtained. Schulberg, Kubiak, and Stulen,[16] for example, derived $E_{\mathrm{H}} = 3.2$ eV by fixing $\nu_{\mathrm{H}} = 10^{13}\ \mathrm{sec}^{-1}$ and $E_{\mathrm{H}} = 1.6$ eV on the basis of the same data set when they considered ν_{H} as a free parameter. If we were to fix ν_{H} at $10^{13}\ \mathrm{sec}^{-1}$ the experimental data could not be fitted. Part of these discrepancies in E_{H} are likely to result from inaccurate temperature measurements. As can be seen from Eqs. (4) and (7) the hydrogen coverage $f_{\mathrm{H}}(T)$ depends on T in a double exponential fashion. This critical dependence requires a very accurate temperature measurement, indeed, if one is to calculate E_{H} from a hydrogen desorption experiment. The Raman line position used here provides this accurate temperature and thus a reliable value for E_{H}.

B. The kinetics of reconstruction

The diamond (111) surface converts from an unreconstructed (1×1) unit mesh to a (2×1) reconstruction upon annealing. We have quantified this phase transition in Figs. 3(b) and 4(b) by measuring the intensity of the half-order LEED spots relative to that of the full-order ones and by the relative intensity of the C $1s$ surface component S_{C} that is due to π-bonded surface atoms. Both ratios saturate for the isothermal annealing sequence and so does the LEED intensity ratio for the isochronal annealing. We take the saturated values to represent the fully reconstructed surface and intermediate values to represent partially reconstructed surfaces such that the normalized relative intensity of the half-order LEED spots equals f_R, the fraction of surface atoms participating in the reconstruction. This implies that the first-order LEED intensities do not vary substantially as one goes through the phase transition. It requires further that reconstructed domains smaller than the typical coherence width of the incident electron beam ($\sim$100 Å) constitute only a small fraction of the total reconstructed area. Both criteria appear to be fulfilled as judged by the close correspondence in the development of half-order LEED spot intensities and S_{C} intensities because the latter constitute a local probe of the π-bonded atoms.

For the sake of our further analysis both intensity ratios (only LEED for temperatures above 1150 K in the isochronal annealing) are fitted to an analytical expression to be discussed later. The fit is shown by the solid lines in Fig. 3(b) and the hatched band in Fig. 4(b).

So far we have considered surface atoms bonded to H and those involved in the π-bonded chain reconstruction. In general, there will also be a fraction of atoms during the annealing process that fall in neither of these two categories but have instead a dangling bond. The role of dangling bonds in the surface phase transitions of diamond has not been considered in earlier studies. The main reason might be that none of the commonly employed surface probes can detect dangling bonds. In this study a sizable concentration of dangling bonds is required in an intermediate temperature or annealing time regime where the fraction f_{H} of surface atoms bonded to hydrogen and the fraction f_R of atoms involved in the (2×1) reconstruction do not add up to unity as shown in Fig. 6. In Fig. 6 f_R is obtained from the fit results in Figs. 3(b) and 4(b), and f_{H} from those of Figs. 3(c) and 4(c). The cross hatching indicates the upper and lower limits in the hydrogen coverage due to the uncertainty of the first data point in Fig. 3(c) (shown by the bar) and an upper limit for the contribution of C-H_x ($x \geqslant 2$) units to χ. The dangling bond coverage f_D, finally, follows from the area conservation:

$$f_{\mathrm{H}} + f_D + f_R = 1. \tag{8}$$

The crucial feature in Fig. 6(a) is that the hydrogen coverage has dropped to about 30% of a monolayer before the reconstruction starts. This requires that the dangling bond density increases to a maximum value of about 70% of a monolayer before it drops again as the (2×1) reconstruction consumes more and more of them in π-bonded chains. The same analysis applied to the varied temperature annealing in Fig. 6(b) gives a picture for the contributions of f_{H}, f_D, and f_R as a function of temperature that agrees quantitatively with that of Fig. 6(a). The hydrogen coverage has to drop to almost 30% of a monolayer before the reconstruction starts and the maximum dangling bond coverage is consequently also about 70%.

Given this result, we describe the surface transformation during annealing as a two-step process. First, C—H bonds convert into dangling bonds with a rate corresponding to Eq.

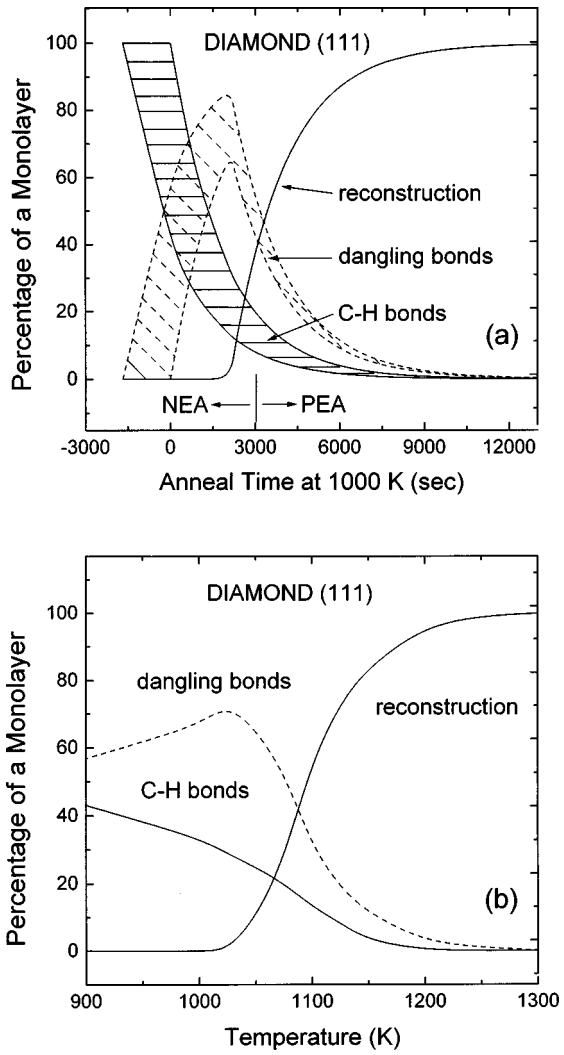

FIG. 6. Evolution of hydrogen, dangling bond, and reconstruction coverage as a function of annealing time (a) and annealing temperature (b). The hatched area in (a) represents uncertainties in hydrogen and dangling bond coverages. The solid line for the reconstruction in (b) corresponds to the smoothed average of the shaded band in Fig. 4(b).

(4). In a second step atoms with dangling bonds transform into surface atoms that participate in the reconstruction. The rate of reconstruction may thus be written as

$$\frac{df_R}{dt}=F(f_D,f_{\mathrm{H}},T). \tag{9}$$

The transformation rate is obviously a function not only of f_D but also of f_{H} because reconstruction sets in only after f_{H} has dropped below ~30%. The rate function F is also thermally activated as judged by the temperature dependence of the (2×1) reconstruction and we thus start with the simplest possible ansatz for the reconstruction rate:

$$\frac{df_R}{dt}=B\Theta(f_{\mathrm{H,crit}}-f_{\mathrm{H}})f_D, \tag{10}$$

with $B=\nu_R e^{-a/kT}$ and the Heaviside function Θ takes into account that the hydrogen coverage has to drop below a critical value $f_{\mathrm{H,crit}}$ before reconstruction sets in. Combining Eq. (10) with Eq. (4) and the area conservation condition Eq. (8) yields for the isothermal annealing experiment

$$f_R(t)=1-(1+\beta e^{-A(T)t_0})e^{-B(T)(t-t_0)}+\beta e^{-A(T)t} \tag{11}$$

for the fraction of surface atoms that participate in the reconstruction. The parameter β equals $\beta=B(T)f_{\mathrm{H}}(0)/[A(T)-B(T)]$ provided the two transformation rates A and B are not equal. Equation (11) involves first the transformation from H-terminated to dangling bond atoms (rate constant A) and then the reconstruction of the latter (rate constant B).

The parameter t_0 in Eq. (11) takes the dependence of F on f_{H} into account. The transformation rate df_R/dt vanishes for $t<t_0$ and jumps to $df_R/dt=B(T)f_D$ for $t>t_0$. Thus t_0 accounts in the most simple form for the experimental observation that a reconstruction takes place only after f_{H} has dropped below the critical value $f_{\mathrm{H,crit}}$ of about 0.3 and t_0 is thus given by

$$t_0=-\frac{\ln(f_{\mathrm{H,crit}})}{A(T)}. \tag{12}$$

A recursion formula for $f_{R,i}$ in the case of isochronal annealing steps follows from the same ansatz:

$$\begin{aligned}f_{R,i}=1-&\left(1+\frac{B_i\Theta(f_{\mathrm{H,crit}}-f_{\mathrm{H},i-1})}{A_i-B_i\Theta(f_{\mathrm{H,crit}}-f_{\mathrm{H},i-1})}f_{\mathrm{H},i-1}-f_{R,i-1}\right)\\&\times e^{-B_i\Theta(f_{\mathrm{H,crit}}-f_{\mathrm{H},i-1})\Delta t}\\&+\frac{B_i\Theta(f_{\mathrm{H,crit}}-f_{\mathrm{H},i-1})}{A_i-B_i\Theta(f_{\mathrm{H,crit}}-f_{\mathrm{H},i-1})}f_{\mathrm{H},i-1}e^{-A_i\Delta t},\end{aligned} \tag{13}$$

with A_i, B_i, and Δt having the obvious meaning. Θ again sets the rate of reconstruction equal to zero as long as the hydrogen concentration has not dropped below the critical value $f_{\mathrm{H,crit}}$.

Expression (11) is used to fit the data of Fig. 3(b) and an excellent fit is obtained with $B(1000\,\mathrm{K})=3.4\times10^{-4}\,\mathrm{sec}^{-1}$, $t_0=2100\,\mathrm{sec}$ corresponding to $f_{\mathrm{H,crit}}=0.32$, and the parameter for A as obtained from the H desorption data (see Sec. IV A). The reconstruction coverage f_R as a function of temperature in the course of the isochronal annealing sequence was calculated using Eq. (13). The results are given by the shaded band in Fig. 4. For these simulations we assumed that the reconstruction rate B jumps to finite value at 1030 K, i.e., at a point where $f_{\mathrm{H}}=f_{\mathrm{H,crit}}$ according to the analysis of the χ values in terms of hydrogen coverage as explained above. The shaded band covers couples ν_R and a between ($3\,\mathrm{sec}^{-1}$, 0.8 eV) and ($1.3\times10^4\,\mathrm{sec}^{-1}$, 1.5 eV) such that the conversion rate constant $B(1000\,\mathrm{K})=3.4\times10^{-4}\,\mathrm{sec}^{-1}$ as derived from the isothermal annealing experiment.

The other study of this phase transition we are aware of is that of Graupner *et al.*,[20] who used the relative intensity of the S_{C} surface component as a measure of π-bonded C atoms that are participating in the reconstruction. They obtained values of ν_R and a of $7.5\times10^{12}\,\mathrm{sec}^{-1}$ and $3.4\pm0.4\,\mathrm{eV}$, respectively, which are considerably larger than those derived here. They did not, however, distinguish between the surface reconstruction and hydrogen desorption and thus ascribed a single activation energy to both processes.

In both annealing sequences the reconstruction is completed at 1000 K (isothermal annealing) or 1150 K (isochro-

nal) which is almost 300 K lower than the temperature quoted in the literature.[20,32,33] Aside from the rather long annealing time required during isothermal annealing this difference is in our opinion mainly due to the more accurate temperature measurement employed here.

Clearly, the reconstruction involves the concerted movement of more than one atom and therefore first-order kinetics to describe this process is bound to be wrong. Despite the good description of both annealing sequences by Eqs. (11) and (13) we are therefore reluctant to identify a with the activation energy necessary to convert a surface atom with a dangling bond into a member of the π-bonded chains that constitute the (2×1) reconstruction. The introduction of a critical hydrogen concentration in Eq. (10) remedies to some extent the gross oversimplification of assuming first-order kinetics for the (1×1) to (2×1) reconstruction because it ensures that the (111) surface does not start to reconstruct before a critical concentration of dangling bonds $f_{D,\mathrm{crit}}$ has been created. The value of $f_{D,\mathrm{crit}}=1-f_{\mathrm{H,crit}}$ as obtained in the fit in conjunction with the hydrogen desorption kinetics from Eq. (12) is $f_{D,\mathrm{crit}}=0.68$. Hamza, Kubiak, and Stulen[27] also reported a hydrogen coverage below $\sim$20% as a necessary condition for the commencement of reconstruction on the diamond (111) surface.

The π-bonded chain as a structural model for the (2×1) reconstruction requires a substantial rebonding of surface atoms with the main result that atoms that used to be next nearest neighbors are nearest neighbors after reconstruction. Clearly, this concerted movement of more than one atom requires the observed 68% of dangling bonds before the reconstruction sets in and leads thus to the delay of surface reconstruction compared with hydrogen desorption.

C. Surface band diagrams

Based on the previous discussion of our results we can identify three distinct phases of the diamond (111) surface: (i) the unreconstructed hydrogen-terminated (1×1):H surface; (ii) the (2×1) reconstructed phase obtained after prolonged annealing at 1000 K (called HT-I for further reference); and (iii) the (2×1) phase reached after 1400 K of annealing (HT-II). Surface band diagrams for these three surfaces have been constructed as shown in Fig. 7.

Changes in band bending were directly measured with an accuracy of ±0.06 eV through the binding energy of the C $1s$ bulk component as described above. For the HT-I surface the absolute value of E_F-E_V at the surface indicated by the right-hand side ordinate of Fig. 3(a) was obtained via Eq. (1) using the saturation value of the work function $\phi=4.97$ eV and the electron affinity $\chi=0.38$ eV. This procedure is more reliable than estimating the valence-band maximum E_V from UP spectra as it is commonly done.[11,32] Once E_F-E_V has been determined all other surface positions of E_F with respect to E_V follow with an accuracy of ±0.06 eV from changes of the binding energy of the C $1s$ component. As a side product of this analysis we obtain the binding energy of the C $1s$ bulk component relative to E_V as 284.13 ± 0.08 eV.

The result of the foregoing analysis may be summarized for the B-doped type-IIb diamond (111) surfaces as follows. The hydrogen-terminated (1×1) surface has a negative electron affinity of -1.27 eV and a downward band bending of 0.36 eV which results in a hole depletion layer.

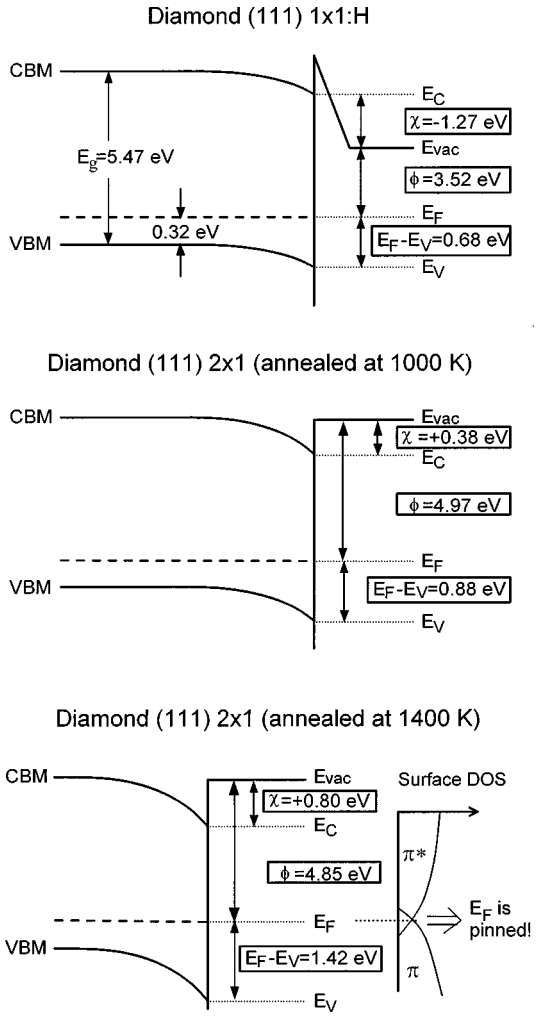

FIG. 7. Band diagram of p-type IIb single crystal diamond at the (111) surface. Upper panel: hydrogen-saturated unreconstructed diamond (111) surface with negative electron affinity. Middle panel: hydrogen-free (2×1) reconstructed diamond (111) surface with positive electron affinity (HT-I phase). The surface was isothermally annealed at 1000 K for 9000 sec. Lower panel: hydrogen-free (2×1) reconstructed diamond (111) surface with positive electron affinity after the surface was annealed at 1400 K for 600 sec (HT-II phase). A schematic band diagram for the surface Fermi level pinning by graphitization is drawn next to the band diagram of the HT-II phase. The semimetallic density of states (DOS) of the graphitic patches consisting of overlapping π and π^* states is indicated.

After hydrogen desorption the (2×1) reconstructed surface phase HT-I is characterized by a small positive electron affinity ($\chi=+0.38$ eV) and a downward band bending of 0.56 eV at the surface (Fig. 7, middle panel). On account of the large band bending and the small positive electron affinity this surface exhibits so-called *effective* NEA. This means that the bulk CBM lies 0.18 eV above the vacuum level. However, this *effective* NEA is not expected to lead to a significantly enhanced electron emission because conduction electrons are unlikely to cross the rather wide depletion layer (150 nm) by ballistic transport. Our experimental values for χ for the NEA and PEA surface are reasonably well repro-

duced by pertinent calculations of Rutter and Robertson[34] who obtain -2.0 and $+0.35$ eV for the two (111) surfaces, respectively.

The second stable high-temperature (111) surface phase HT-II has a larger electron affinity ($\chi = +0.8$ eV) and also a larger downward band bending that now reaches a value of 1.1 eV. Also this surface still exhibits effective NEA.

As discussed earlier, for the isochronal annealing sequence the relative intensity of the surface component S_C continues to increase further above 1150 K, i.e., after the surface reconstruction from (1×1) to (2×1) is completed as judged by the intensity of the half-order LEED spots (compare Fig. 4). This further increase in S_C at high temperature was earlier ascribed to a gradual graphitization of the surface.[20] It was argued that the graphitization takes place locally and involves the successive delamination of patches of π-bonded graphitic layers leaving (2×1) reconstructed areas in between. This explains why the intensity of S_C increases beyond that characteristic for the (2×1) reconstructed surface while the LEED pattern is still that of the (2×1) surface. In fact, a growing background of incoherently scattered intensity in the diffraction pattern as T rises above 1150 K must be ascribed to the fraction of disordered, graphitic surface area that grows at the expense of the ordered, (2×1) reconstructed one. A partial graphitization is sufficient to account for the new pinning position of E_F at 1.42 eV above E_V for $T\sim1400$ K (compare Fig. 7).

There is general agreement in the literature that the hydrogenated (111) surface has NEA and a downward band bending on *p*-type diamond that turns into PEA upon reconstruction while the downward band bending increases. However, there is considerable scatter in the values given for the initial surface Fermi level position (0.4 to 1.0 eV above E_V) as well as its final position (1.0 to 1.6 eV).[10,11] Considering our new results the latter is most likely due to the fact that no distinction was made between the two electronically different reconstructed surface phases. This might also be the reason for the electron affinity of $+0.5$ eV quoted by Bandis and Pate[10] for the reconstructed (111) surface which lies intermediate between our surface HT-I ($\chi = +0.38$ eV) and HT-II ($\chi = +0.8$ eV) values.

A surface charge density (in units of elementary charge) of $+2.7\times10^{11}\,\mathrm{cm}^{-2}$ is needed in the Schottky approximation to account for the observed band bending on our samples with a B concentration of $10^{16}\,\mathrm{cm}^{-3}$. This surface charge is easily accommodated by a slight reduction in the occupation of the normally filled π states of the graphitic surface patches. In fact, we expect that for a sufficiently high coverage with graphitic patches E_F will effectively be pinned at or around the position measured here as indicated in the lower panel of Fig. 7. This scenario is supported by the observation that $E_{\mathrm{vac}} - E_F = 4.85$ eV on the HT-II surface is very close to the work function of graphite ($\phi = 5.0$ eV).

V. SUMMARY

A change in electron affinity χ from -1.27 eV for the hydrogen-covered (111) surface to $+0.38$ eV for the hydrogen-free (2×1) reconstructed surface has been measured. The variation in χ with temperature could be accounted for quantitatively by considering the potential step associated with the dipole layer set up by the partially ionic C^-—H^+ bonds at the surface provided the depolarization of the dipoles is properly taken into account.

Based on the correlation between χ and the hydrogen coverage a clear distinction between hydrogen desorption and reconstruction has been established. Hydrogen desorption is well described by a first-order process with an activation energy of 1.25 ± 0.2 eV and a prefactor of $5.4\times10^{-4}\,\mathrm{sec}^{-1}$. The onset of reconstruction is obviously topologically constrained and requires a critical concentration of atoms with dangling bonds. Once this condition is incorporated into the rate equations the phase transition from a hydrogen-free unreconstructed to a (2×1) reconstructed surface is also well described by a first-order process with a critical concentration of dangling bond $f_{D,\mathrm{crit}} = 0.68$, a prefactor $\nu_R = 4\times10^{2\pm2}\,\mathrm{sec}^{-1}$; and an ''activation energy'' $a = 1.2\pm0.4$ eV. We concede that the last two quantities are at present mere parameters that are used to fit the time and temperature dependence of the reconstruction. Without further evidence the parameter α should therefore not be taken as the activation energy that is required to transform a dangling bond into a member of a π-bonded chain.

For the hydrogen-free (2×1) surface we identified two distinct phases that are stable over certain temperature ranges but differ in their band energies at the surface without changes in reconstruction. The ''low-temperature'' phase is reached after isothermal annealing at 1000 K. It has the aforementioned electron affinity χ of $+0.38$ eV and a downward band bending at the surface of 0.56 eV, i.e., 0.2 eV larger than the hydrogenated (1×1) surface. Taking the surface to 1400 K results in the high-temperature (2×1) phase for which both electron affinity ($\chi = +0.8$ eV) and downward band bending (1.1 eV) have further increased. The analysis of the C 1*s* core level spectra indicates that the high-temperature phase is associated with an incipient graphitization of the diamond (111) surface.

ACKNOWLEDGMENTS

The authors thank M. Stammler and K. Janischowsky for the plasma preparation of the diamond surfaces and R. Graupner for helpful discussions. This work was supported by the Deutsche Forschungsgemeinschaft under Contract No. DFG Le 634/5-3 and carried out under the auspices of the trinational ''D-A-CH'' cooperation of Germany, Austria, and Switzerland on ''Synthesis of Superhard Materials.''

[1] J. J. Lander and J. Morrison, Surf. Sci. **4**, 241 (1966).
[2] P. G. Lurie and J. M. Wilson, Surf. Sci. **65**, 453 (1977).
[3] C.-L. Cheng, H.-C. Chang, J.-C. Lin, K.-J. Song, and J.-K. Wang, Phys. Rev. Lett. **78**, 3713 (1997).
[4] H. Sasaki and H. Kawarada, Jpn. J. Appl. Phys., Part 2 **32**, L1771 (1993).
[5] Y. L. Yang and M. P. D'Evelyn, J. Vac. Sci. Technol. A **10**, 978 (1992).
[6] B. D. Thoms and J. E. Butler, Surf. Sci. **328**, 281 (1995).
[7] K. C. Pandey, Phys. Rev. B **25**, 4338 (1982).
[8] R. Graupner, M. Hollering, A. Ziegler, J. Ristein, and L. Ley, Phys. Rev. B **55**, 10 841 (1997).

[9] R. J. Nemanich, P. K. Baumann, M. C. Benjamin, S. W. King, J. van der Weide, and R. F. Davis, Diamond Relat. Mater. **5**, 790 (1996).
[10] C. Bandis and B. Pate, Phys. Rev. B **52**, 12 056 (1995).
[11] J. Himpsel, D. E. Eastman, P. Heimann, and J. F. van der Veen, Phys. Rev. B **24**, 7270 (1981).
[12] J. B. Cui, J. Ristein, and L. Ley, Phys. Rev. Lett. **81**, 429 (1998).
[13] F. J. Himpsel, J. A. Knapp, J. A. Van Vechten, and D. E. Eastman, Phys. Rev. B **20**, 624 (1979).
[14] B. B. Pate, P. M. Stefan, C. Binns, P. J. Jupiter, M. L. Shek, I. Lindau, and W. E. Spicer, J. Vac. Sci. Technol. **19**, 349 (1981).
[15] A. V. Hamza, G. D. Kubiak, and R. H. Stulen, Surf. Sci. **237**, 35 (1990).
[16] M. T. Schulberg, G. D. Kubiak, and R. H. Stulen, in *Novel Forms of Carbon*, edited by C. L. Renschler, J. J. Pouch, and P. M. Cox, MRS Symposia Proceedings No. 270 (Materials Research Society, Pittsburgh, 1992), p. 401.
[17] R. E. Thomas, R. A. Rudder, and R. J. Markunas, J. Vac. Sci. Technol. A **10**, 2451 (1992).
[18] Y. L. Yang, L. M. Struck, L. F. Sutcu, and M. P. D'Evlyn, Thin Solid Films **225**, 203 (1993).
[19] K. Bobrov, B. Fisgeer, H. Schechter, M. Folman, and A. Hoffman, Diamond Relat. Mater. **6**, 736 (1997).
[20] R. Graupner, F. Maier, J. Ristein, L. Ley, and Ch. Jung, Phys. Rev. B **57**, 12 397 (1998).
[21] B. D. Thoms, M. S. Owens, J. E. Butler, and C. Spiro, Appl. Phys. Lett. **65**, 2957 (1994).
[22] O. M. Küttel, K. Diederich, E. Schaller, O. Carnal, and L. Schlapbach, Surf. Sci. **337**, L812 (1995).
[23] J. B. Cui, K. Amtmann, J. Ristein, and L. Ley, J. Appl. Phys. **83**, 7929 (1998).
[24] W. Thomson, Philos. Mag. **46**, 82 (1898).
[25] J. Schäfer, J. Ristein, L. Ley, and H. Ibach, Rev. Sci. Instrum. **64**, 653 (1993).
[26] J. Ristein, W. Stein, and L. Ley, Phys. Rev. Lett. **78**, 1803 (1997).
[27] V. Hamza, G. D. Kubiak, and R. H. Stulen, Surf. Sci. **206**, L833 (1988).
[28] J. Topping, Proc. R. Soc. London, Ser. A **114**, 67 (1927).
[29] Values of α for CH_2 ($1.64\times10^{-40}\,Asm^2/V$) and CH_3 ($1.88\times10^{-40}\,Asm^2/V$) have been calculated by K. M. Gough, J. Chem. Phys. **91**, 2424 (1989).
[30] The possibility that the surface is partially covered by C-H_3 units instead of C-H does not alter our results substantially because the perpendicular component of the dipole moment of C-H_3 equals that of C-H to first order.
[31] T. Nishimori, H. Skamoto, Y. Takakuwa, and S. Kono, J. Vac. Sci. Technol. A **13**, 2781 (1995).
[32] B. Pate, Surf. Sci. **165**, 83 (1986).
[33] R. P. Chin, J. Y. Huang Y. R. Shen, T. J. Chuang, H. Seki, and M. Buck, Phys. Rev. B **45**, 1552 (1992).
[34] M. J. Rutter and J. Robertson, Phys. Rev. B **57**, 9241 (1998).